Air flow optimization for drinking water production through air dehumidification

Marco Bortolini*, Mauro Gamberi, Alessandro Graziani**, Alessandro Persona**, Francesco Pilati**, Alberto Regattieri***

** Department of Industrial Engineering, University of Bologna,*

Viale Risorgimento 2, 40136 Bologna – Italy (marco.bortolini3@unibo.it, alberto.regattieri@unibo.it)

*** Department of Management and Engineering, University of Padova,*

Stradella San Nicola 3, 36100 Vicenza – Italy (mauro.gamberi@unipd.it, alessandro.graziani6@unibo.it, alessandro.persona@unipd.it, pilati@gest.unipd.it).

Abstract: Drinking water availability is one of the emerging challenges of the 21st century. Different approaches have been investigated as possible sources of water for arid regions. Atmospheric water vapor processing is a developing approach whose aim is to cool air to condensate the water available in the atmospheric moisture. Air dehumidification allows obtaining pure drinking water for geographical regions far from sea, rivers or lakes.

This paper presents the optimization of a refrigeration system for drinking water production through air dehumidification. The system uses a fan to force the atmospheric air through an heat exchanger, in which it is cooled. The water vapor condensates on the cooled heat exchanger surfaces and it is collected by gravity in a tank.

The system aim is to condensate the maximum water quantity achievable for every atmospheric air condition, represented by temperature and humidity. Thus, a mathematical model is proposed to determine the optimal atmospheric air flow that maximizes the condensed water production for every atmospheric air condition. An experimental campaign is set up to validate the proposed model. Experimental test results show that the mathematical model accurately predicts the drinking water production (error between +4.1% and -5.6%). Thus, for every atmospheric air condition, the optimal air flow value and the related condensed water production are determined. Relative humidity greater than 70% and temperature higher than 35°C guarantee more than 1.0 liter of drinking water produced per hour and kW of refrigeration power installed.

Keywords: drinking water production, atmospheric water vapor processing, air flow optimization.

1. Introduction and literature review.

The United Nations define the improvement of drinking water access as one of the Millennium Development Goals. Nowadays, about 768 million people around the world have no access to any source of drinking water (United Nations, 2013), and by 2025 the number of people that will live in water-stressed countries is expected to rise up to 3 billion (Anbarasu and Pavithra, 2011). North Africa and Middle-East, in particular, have to face with severe water shortage. 15% of their population, indeed, has no access to any source of clean and fresh water (Miller, 2003).

Several technologies, decentralized small-scale in particular, are designed to produce drinking water in arid regions (Shanmugam et al., 2004).

- Rainwater harvesting is the technique adopted to collect rainwater from rooftops or land surfaces and store it in natural or artificial reservoirs (Helmreich and Horn, 2009).
- Desalination removes salt and other minerals from saline water to produce drinking water (Ghaffour et. al, 2013). Two are the processes traditionally exploited. Evaporation distils seawater using a heat source, whereas membrane process separates the drinking water from a saline concentrate (Narayan et. al, 2010).
- Atmospheric water vapor processing (AWVP) is the technique to extract water molecules from the atmospheric moisture, exploiting the water phase change from vapor to liquid (Wahlgren, 2001). Compared to the aforementioned technologies, AWVP represents a significant opportunity to produce drinking water even in regions far from natural water basins or affected by sporadic rainfall (Mezher et. al, 2011). The water contained in the earth atmospheric

moisture is, indeed, over 12.9 billion cubic meter (Gleick, 1996 and Gleick, 2000).

Considering AWVP, three are the processes traditionally adopted to produce drinking water from the atmospheric moisture.

- Atmospheric vapor concentration uses desiccants to extract water from air by means of vapor pressure reduction that determines a flow of water molecule toward the desiccant surface (Gad et. al, 2001). The desiccants are classified in absorbents and adsorbents (Ji et al., 2007). The formers change chemically or physically during the water molecule absorption, the latters no (Abualhamayel and Gandhidasan, 1997).
- Atmospheric controlled convection purpose is to induce air currents in tall tower structure from high altitude where the condensation occurs (Starr et al., 1972).
- Atmospheric moisture condensation forces an air flow to pass through surfaces cooled by a refrigeration system. The air temperature reduction below the dew point determines the atmospheric moisture condensation. Thus, the produced water is collected in tanks.

Several authors investigate the relation between the water production and the atmospheric air conditions, namely temperature, pressure and relative or absolute humidity, for atmospheric moisture condensation process. Milani et al. (2011) propose a relation between the atmospheric air conditions at the entrance of their thermoelectric cooler and the amount of condensable water. Scrivani and Bardi (2008) evaluate the quantity of drinking water that can be obtained by a solar powered system in Morocco, Jordan and Lebanon. Nevertheless, both these authors do not investigate how the refrigeration system operating parameters affect the water production. Carrington and Liu (1995) and Khalil (1993), instead, suggest that the air flow value significantly affects the condensed water quantity. Jradi et al. (2011) investigate the relation between the air flow and the water production for a thermoelectric system installed in Lebanon. Habeebullah (2009) estimates the condensed water quantity for different air flows for a refrigeration system installed in Saudi Arabia. However, the optimal air flow value suggested by both the authors is constant during the operating period, thus it does not consider the atmospheric air conditions variation.

This paper proposes a mathematical model to determine the optimal air flow of a refrigeration system for AWVP that maximizes the condensed water production considering the atmospheric air conditions, namely temperature, pressure and relative or absolute humidity. The model is validated through an experimental campaign that exploits a refrigeration system to produce drinking water simulating the atmospheric air conditions required. Furthermore, the validated model is used to determine the optimal air flow that maximizes the water production for every atmospheric air condition between 10°C and 50°C for temperature and between 6 and 85 $g_{H2O}/kg_{dry\ air}$ for absolute humidity.

The remainder of this paper is organized as follows. The next Section 2 proposes the AWVP mathematical model. Section 3 presents the experimental campaign used to validate the model, together with the refrigeration system and the test procedure adopted. Section 4 illustrates the experimental campaign results and the optimal air flows determined by the AWVP model. Finally Section 5 presents the paper conclusions and suggests further research opportunities.

2. Atmospheric water vapor processing mathematical model.

The process to produce drinking water by means of atmospheric moisture condensation is described in this Section, together with its mathematical formulation.

A volumetric flow $\dot{v}_a$ of air at atmospheric conditions defined by temperature T_a, pressure P_a and absolute humidity ω_a (or relative one φ_a) is forced by a fan to pass through a cooled heat exchanger. The system refrigeration power RP is used to remove the sensible Q_s and the latent Q_l heat from the air flow (Eq. 1).

$$RP = Q_s + Q_l \tag{1}$$

Q_s represents the refrigeration power component required to lower the air temperature from atmospheric conditions T_a to post-condensation one T_c (Eq. 2), whereas Q_l accounts for the refrigeration power necessary for air dehumidification from ω_a to ω_c absolute humidity (Eq. 3) and the related condensed water production $\dot{q}_c$ (Eq. 4).

$$Q_s = \dot{v}_a \cdot \rho_{air} \cdot c_{air} \cdot (T_a - T_c) \tag{2}$$

$$Q_l = \dot{v}_a \cdot \rho_{air} \cdot r_{H2O} \cdot (\omega_a - \omega_c) \tag{3}$$

$$\dot{q}_c = \dot{v}_a \cdot \rho_{air} \cdot (\omega_a - \omega_c) \tag{4}$$

The air at post-condensation state is in saturation condition. Thus, exploiting Buck (1981) experimental equation, it is possible to determine a relation between the temperature T_c and the absolute humidity ω_c of air in post-condensation state. It is necessary to consider Buck experimental equation (Eq. 5), water vapor and dry air equation of state (Eq. 6 and Eq. 7) and Dalton's law (Eq. 8). Using Eq. 6 and Eq. 7 it is possible to determine ω_c as a function of P_a and T_c (Eq. 9). Combining Eq. 9 with Eq. 5 T_c can be expressed as a function of ω_c and P_a (Eq. 10). Furthermore, Eqs. 5-8 enable to determine the atmospheric air flow density ρ_{air} as a function of the atmospheric air conditions (Eq. 11).

Combining Eqs. 1-4 and Eq. 10, Eq. 12 represents the relation between the air flow $\dot{v}_a$ and the post-condensation absolute humidity ω_c considering the system refrigeration power and the atmospheric air conditions. Eq. 4 is rearranged to define ω_c as a function of $\dot{v}_a$, $\dot{q}_c$ and the atmospheric air conditions (Eq. 13). Using Eq. 13 to substitute ω_c in Eq. 12 it is possible to define Eq. 14. It represents the relation between the air flow $\dot{v}_a$ and the condensed water quantity $\dot{q}_c$ for a refrigeration system of refrigeration power RP operating at atmospheric air conditions T_a, P_a and ω_a (or φ_a). Eq. 15, similarly, relates the post-condensation air temperature T_c to the atmospheric air inflow $\dot{v}_a$. Eq. 14 enables to determine the optimal air flow that maximizes the condensed water production for every atmospheric air conditions and system refrigeration power. Accordingly to this purpose, Eq. 15 estimates the air temperature at post-condensation state for the optimal air flow. Both Eqs. 14 and 15 are non-linear, thus a iterative procedure is required to solve them. The next Section 3 presents the experimental campaign used to validate Eqs. 14 and 15, together with the refrigeration system and the test procedure adopted.

The definitions of the variables and the parameters of the equations proposed in this Section are presented in the Appendix A, whereas the values of the parameters are listed in the Appendix B.

$$P_{H2O} = x \cdot (1 + A + B \cdot P_a) \cdot e^{\frac{y \cdot T_c}{z+T_c}} = D \cdot e^{\frac{y \cdot T_c}{z+T_c}} \tag{5}$$

$$P_{H2O} \cdot V = n_{H2O} \cdot R \cdot T_c = n_{H2O} \cdot \frac{m_{H2O}}{m_{H2O}} \cdot R \cdot T_c = \frac{M_{H2O}}{m_{H2O}} \cdot R \cdot T_c \tag{6}$$

$$P_{air} \cdot V = n_{air} \cdot R \cdot T_c = n_{air} \cdot \frac{m_{air}}{m_{air}} \cdot R \cdot T_c = \frac{M_{air}}{m_{air}} \cdot R \cdot T_c \tag{7}$$

$$P_a = P_{H2O} + P_{air} \tag{8}$$

$$\omega_c = \frac{M_{H2O}}{M_{air}} \cdot f = \frac{m_{H2O}}{m_{air}} \cdot \frac{P_{H2O}}{P_a - P_{H2O}} \cdot f = \frac{m_{H2O}}{m_{air}} \cdot \frac{D \cdot e^{\frac{y \cdot T_c}{z+T_c}}}{P_a - D \cdot e^{\frac{y \cdot T_c}{z+T_c}}} \cdot f \tag{9}$$

$$T_c = \frac{z \cdot ln\left[\frac{\frac{\omega_c}{f} \cdot \frac{m_{air}}{m_{H2O}} \cdot P_a}{\left(1 + \frac{\omega_c}{f} \cdot \frac{m_{air}}{m_{H2O}}\right) \cdot D}\right]}{y - ln\left[\frac{\frac{\omega_c}{f} \cdot \frac{m_{air}}{m_{H2O}} \cdot P_a}{\left(1 + \frac{\omega_c}{f} \cdot \frac{m_{air}}{m_{H2O}}\right) \cdot D}\right]} \tag{10}$$

$$\rho_{air} = \frac{P_a - \varphi_a \cdot D \cdot e^{\frac{y \cdot T_a}{z+T_a}}}{\frac{R}{m_{air}} \cdot T_a} \tag{11}$$

$$RP = \dot{v}_a \cdot \rho_{air} \cdot c_{air} \cdot \left\{ T_a - \frac{z \cdot ln\left[\frac{\frac{\omega_c}{f} \cdot \frac{m_{air}}{m_{H2O}} \cdot P_a}{\left(1 + \frac{\omega_c}{f} \cdot \frac{m_{air}}{m_{H2O}}\right) \cdot D}\right]}{y - ln\left[\frac{\frac{\omega_c}{f} \cdot \frac{m_{air}}{m_{H2O}} \cdot P_a}{\left(1 + \frac{\omega_c}{f} \cdot \frac{m_{air}}{m_{H2O}}\right) \cdot D}\right]} \right\} + r_{H2O} \cdot \dot{q}_c \tag{12}$$

$$\omega_c = \omega_a - \frac{\dot{q}_c}{\rho_{air} \cdot \dot{v}_a} \tag{13}$$

$$RP = \dot{v}_a \cdot \rho_{air} \cdot c_{air} \cdot \left\{ T_a - \frac{z \cdot ln\left[\frac{\left(\omega_a - \frac{\dot{q}_c}{\rho_{air} \cdot \dot{v}_a}\right) \cdot \frac{m_{air}}{f \cdot m_{H2O}} \cdot P_a}{\left(1 + \left(\omega_a - \frac{\dot{q}_c}{\rho_{air} \cdot \dot{v}_a}\right) \cdot \frac{m_{air}}{f \cdot m_{H2O}}\right) \cdot D}\right]}{y - ln\left[\frac{\left(\omega_a - \frac{\dot{q}_c}{\rho_{air} \cdot \dot{v}_a}\right) \cdot \frac{m_{air}}{f \cdot m_{H2O}} \cdot P_a}{\left(1 + \left(\omega_a - \frac{\dot{q}_c}{\rho_{air} \cdot \dot{v}_a}\right) \cdot \frac{m_{air}}{f \cdot m_{H2O}}\right) \cdot D}\right]} \right\} + r_{H2O} \cdot \dot{q}_c \tag{14}$$

$$RP = \dot{v}_a \cdot \rho_{air} \cdot \left[c_{air} \cdot (T_a - T_c) + r_{H2O} \cdot \left(\omega_a - \frac{m_{H2O}}{m_{air}} \cdot \frac{D \cdot e^{\frac{y \cdot T_c}{z+T_c}}}{P_a - D \cdot e^{\frac{y \cdot T_c}{z+T_c}}} \cdot f \right) \right] \tag{15}$$

3. Experimental campaign.

This Section presents the experimental campaign focused on the validation of the AWVP mathematical model, Eqs. 14 and 15 in particular. Three are the experimental campaign relevant features: the refrigerator system used for water condensation, the control system for input and output signal processing and the test procedure.

3.1. Refrigeration system.

A thermoelectric refrigeration system is designed and crafted for the experimental campaign. A centrifugal fan forces the air flow to pass through a plastic pipe of section A where the air temperature and relative humidity are set to the simulated atmospheric conditions using a heater and a humidifier, respectively. Thus, the air flow passes through a vertical heat exchanger cooled by 20 thermoelectric packs mounted on two opposite side of the heat exchanger. A thermoelectric pack is made of a couple of thermoelectric cells connected to a fan cooled heat sink. The heat exchanger is thermally insulated by polyurethane films. The condensed water is collected by a funnel and stored in a bottle to avoid water evaporation. Figure 1.a represents the refrigeration system diagram, while Figure 1.b is a picture of it. The refrigeration system component characteristics are listed in Table 1.

3.2. Control system.

The validation of the AWVP mathematical model presented in Section 2 requires to simulate a particular set of atmospheric air conditions at the heat exchanger entrance. The simulated atmospheric air temperature T_a is measured by means of a PT100 termoresistence with ± 0.3°C accuracy, while the simulated atmospheric air relative humidity φ_a is measured using a capacitive humidity sensor with ± 2% accuracy. A real time proportional-integral (PI) close-loop controller uses these data to regulate the heater and the humidifier to set the temperature and humidity values equal to the one required. The air temperature T_e and relative humidity φ_e at the exit of the heat exchanger are measured by means of identical termoresistence and capacitive humidity sensor. The air flow is regulated by the centrifugal fan and its speed S is measured using an anemometer with ± 0.1 m/s accuracy, while the condensed water quantity is weighted by a digital scale with ± 1 g accuracy. The acquisition of the sensor signals, the data processing and the PI controller are provided with a customized and easy-use real-time interface developed in the Labview™ integrated development environment. Figure 2 shows the front panel of the monitoring and control tool.

3.3. Test procedure.

Aim of the experimental campaign is to measure the condensed water quantity and the post-condensation air temperature for several air flow values simulating a particular set of atmospheric air conditions. The following test procedure is used for this purpose.

- Air flow speed regulation to the required value.
- Setup of the simulation atmospheric air conditions.
- Condensed water quantity measurement at interval of 10 minutes.
- Measurement of air conditions at heat exchanger exit.
- Evaluation of air conditions in post-condensation state and by-pass factor. Air conditions at the heat exchanger exit (T_e, φ_e) differ to the post-condensation one (T_c, φ_c). Part of the air blown by the fan is not affected by the heat exchange. Thus, its temperature and humidity does not vary. This percentage is defined bypass factor F. Most of the air blown $(1-F)$, instead, is distinguished by post-condensation conditions equal to T_c, φ_c. The air conditions measured at the heat exchanger exit T_e, φ_e are determined by the aforementioned air flows mix. Considering that $\varphi_c = 100\%$, T_c can be evaluated through the measurement of $T_a, \varphi_a, T_e, \varphi_e$. The temperature and humidity values of air at atmospheric, heat exchanger exit and post-condensation conditions enable the bypass factor F evaluation.
- Evaluation of the air flow through the following Eq. 16.

$$\dot{v}_a = S \cdot A \cdot (1 - F) \tag{16}$$

- Evaluation of the refrigeration power using Eqs. 1-3 and 11.

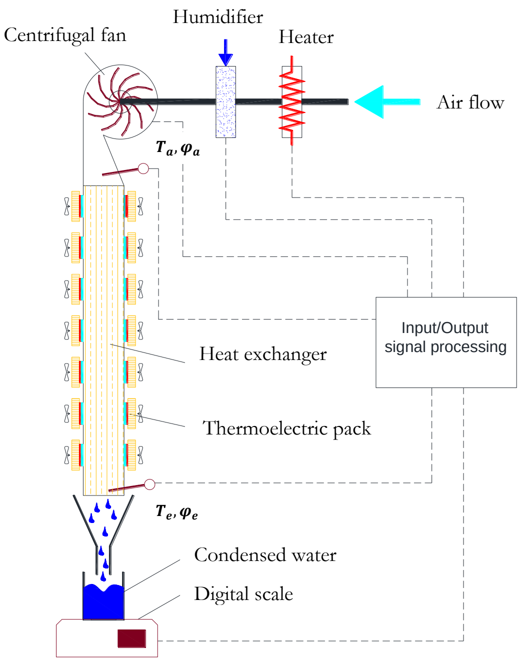

Figure 1.a. Refrigeration system diagram.

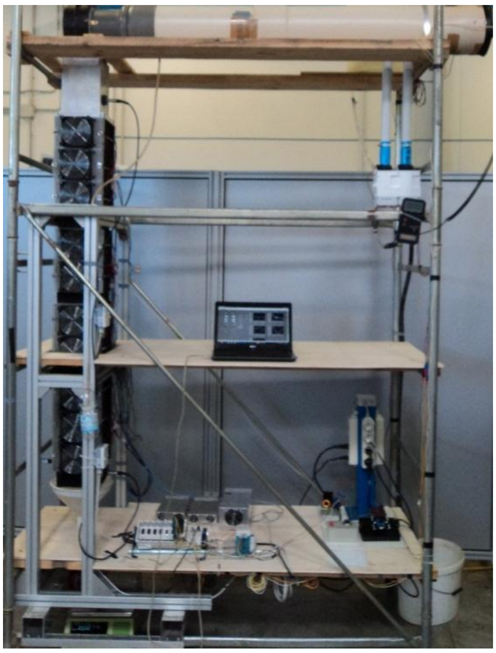

Figure 1.b. Refrigeration system picture.

Table 1. Refrigeration system component characteristics.

Component	Characteristics
Inflow pipe	Length 154 cm, circular section of 298.6 cm^2.
Heater	Resistor, maximum thermal load 700 W.
Humidifier	Ultrasonic humidifier, maximum vaporization capacity 1.2 l/h.
Centrifugal fan	Power requirement 105 W, maximum air flow 320 m^3/h.
Heat exchanger	Height 146 cm, section 160 x 160 mm.
Thermoelectric cell	Area 40 x 40 mm. Specifications for 25°C hot face temperature: maximum absorbable heat 72.0 W, maximum input current 8.5 A, maximum voltage 15.4 V, maximum temperature difference 65°C.

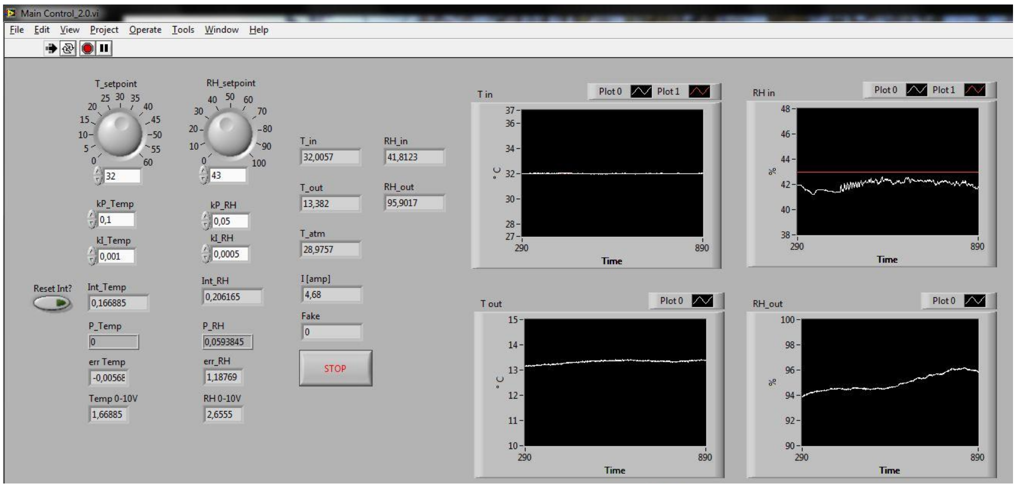

Figure 2. Real-time monitoring and control tool.

4. Results and discussion.

The validation of the AWVP mathematical model through the experimental campaign is presented in this Section. Six different air flow values are tested by the refrigeration system: 57, 73, 88, 100, 115 and 127 m^3/h. The simulating atmospheric air conditions are T_a=32°C, P_a=1010 mbar and ω_a=12.16 $g_{H2O}/kg_{dry\ air}$ (or φ_a=39.5%). For each air flow value the condensed water quantity and the post-condensation air temperature are measured. $\dot{v}_a - \dot{q}_c$ relation is presented in Figure 3.a whereas Figure 3.b proposes $\dot{v}_a - T_c$ relation, both for the AWVP mathematical model and for the experimental campaign. The AWVP model accurately predicts the condensed water and post-condensation temperature values. The difference between the $\dot{q}_c$ measured during the experimental campaign and the one estimated by the model is between +4.1% and -5.6% for each tested air flow value, while the T_c error is between -0.3% and -0.5%. As shown by Figures 3.a and 3.b, for these atmospheric air conditions the optimal air flow differs to the one that maximizes the water production. Indeed, the latter does not represent a feasible system configuration. T_c would be lower the minimum allowed (≅5°C). In this condition, the overcooling refrigeration condensates the atmospheric moisture, but it determines frost formation at heat exchanger due to T_c almost equal or lower than 0°C. For high $\dot{v}_a$, instead, RP is not enough to start the dehumidification process. The heat removed by the air flow does not reduce the atmospheric air temperature below the dew point. Thus Q_l is equal to 0 and no water is produced.

The validated AWVP mathematical model is used to determine the optimal air flow that maximizes the condensed water production for every atmospheric air condition between 10°C and 50°C for T_a and between 6 and 85 $g_{H2O}/kg_{dry\ air}$ for ω_a considering P_a=1013 mbar and RP =1 kW. This Section presents the model results for the feasible $T_a - \omega_a$combinations. As shown in Figure 4, the higher ω_a, the higher the maximum condensed water quantity is, for each T_a value. On the contrary, lower T_a enables a greater water production for the same value of ω_a. For hot and humid atmospheric air conditions, distinguished by $T_a \geq$ 35°C and $\varphi_a \geq$ 70%, the maximum condensed water production varies between 1.00 and 1.42 l/h per kW of refrigeration power installed. Table 2 presents the optimal air flow values for every atmospheric condition. The value range is wide and included between 32 and 466 m^3/h. For each ω_a considered, the lower T_a the greater the optimal air flow value is. As shown in Table 2, this relation is determined by Q_l/RP. The lower T_a the higher Q_l/RP is. Thus, high optimal air flow value enables to exploit this favourable condition and to increase the water production.

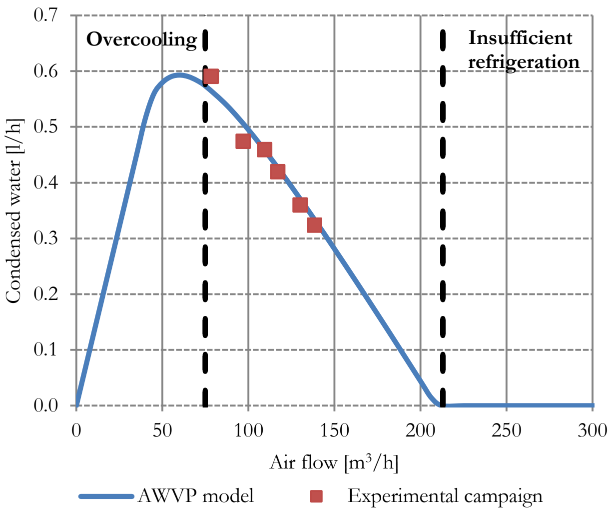

Figure 3.a. $\dot{v}_a - \dot{q}_c$ **relation for** T_a**=32°C,** P_a**=1010 mbar,** ω_a**=12.16** $g_{H2O}/kg_{dry\ air}$ **(or** φ_a**=39.5%) and** RP **=1kW.**

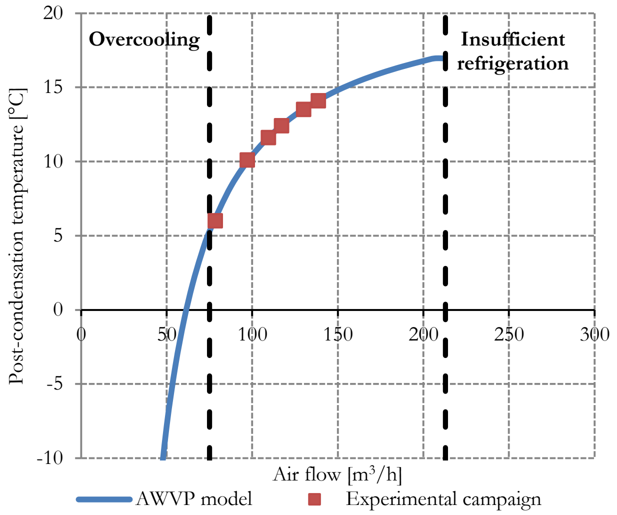

Figure 3.b. $\dot{v}_a - T_c$ **relation for** T_a**=32°C,** P_a**=1010 mbar,** ω_a**=12.16** $g_{H2O}/kg_{dry\ air}$ **(or** φ_a**=39.5%) and** RP **=1kW.**

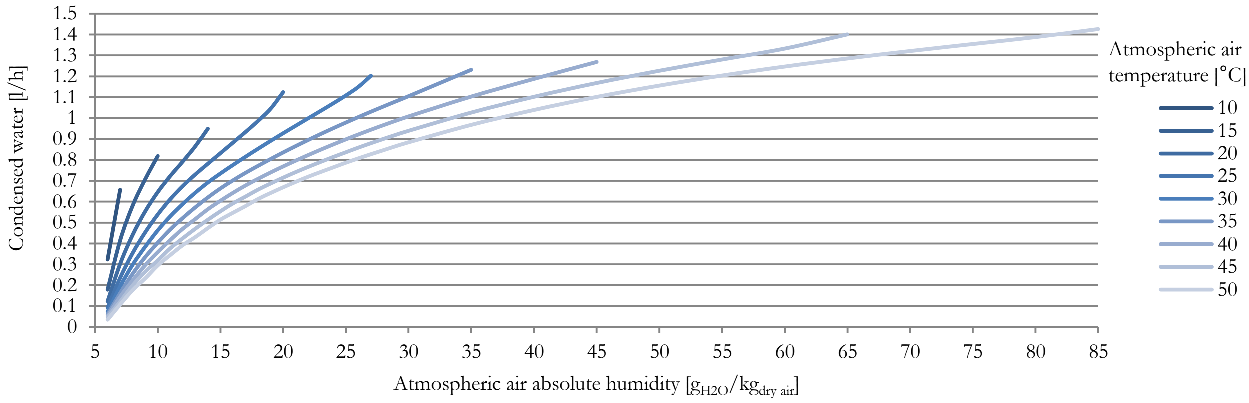

Figure 4. Condensed water for every atmospheric air condition (RP **=1 kW,** P_a**=1013 mbar).**

Table 2. Optimal air flow and Q_l/RP **for every atmospheric air condition (**RP**=1 kW,** P_a**=1013 mbar).**

	Optimal air flow [m³/h]									Q_l/RP								
	T_a [°C]									T_a [°C]								
ω_a [$g_{H2O}/kg_{dry\ air}$]	10	15	20	25	30	35	40	45	50	10	15	20	25	30	35	40	45	50
6	466	260	180	138	112	94	81	71	64	20%	11%	8%	6%	5%	4%	3%	3%	2%
10		215	116	97	83	73	65	59	53		52%	41%	34%	29%	25%	23%	20%	19%
15				88	64	57	52	48	44				53%	46%	42%	38%	35%	32%
20				344	72	54	46	41	38				71%	59%	53%	49%	45%	42%
25					106	58	46	40	35					70%	62%	57%	53%	50%
30						66	47	39	34						70%	64%	59%	56%
35						108	49	39	33						78%	70%	65%	61%
40							54	39	33							75%	70%	66%
45							70	39	32							80%	74%	70%
50								41	32								77%	73%
55								45	32								81%	76%
60								56	32								84%	79%
65								200	33								88%	81%
70									35									83%
75									38									85%
80									46									88%
85									81									90%

5. Conclusions.

This paper presents the optimization of a refrigeration system for drinking water production through air dehumidification. An AWVP mathematical model is proposed to determine the optimal air flow entering the refrigeration system that maximizes the condensed water production for every atmospheric air condition. An experimental campaign is setup to validate the proposed model. A thermoelectric refrigeration system is designed and crafted for the experimental analysis. A control system regulates a heater and a humidifier to simulate the required atmospheric air conditions. Several air flow values are tested and the related condensed water production is measured. The AWVP mathematical model accurately predicts the drinking water production. The difference between the experimental campaign values and the model one is between +4.1% and -5.6%. Thus, the validated AWVP model is used to determine the optimal air flow for every atmospheric air condition between 10°C and 50°C for T_a and between 6 and 85 $g_{H2O}/kg_{dry\ air}$ for ω_a. For hot and humid atmospheric air conditions, distinguished by $T_a \geq 35$°C and $\varphi_a \geq 70\%$, the maximum condensed water production varies between 1.00 and 1.42 l/h per kW of refrigeration power installed.

Further research has to improve the experimental campaign simulating the atmospheric air condition hourly profiles of a specific installation site and implementing an air flow controller. Furthermore, the refrigeration system has to be integrated with a renewable power plant for energy supply. This integrated system has to be optimized to simultaneously minimize the cost and the greenhouse gas emissions per liter of drinking water produced.

References.

Abualhamayel, H. I., Gandhidasan P., (1997). A method of obtaining fresh water from the humid atmosphere. *Desalination,* v. 113, p. 51-63.

Anbarasu, T., Pavithra, S., (2011). Vapour compression refrigeration system generating fresh water from humidity in the air. In *Proceedings of Sustainable Energy and Intelligent Systems (SEISCON 2011)*, Tamil Nadu, India.

Buck, A. L., (1981). New equations for computing vapor pressure and enhancement factor. *Journal of Applied Meteorology,* v. 20, p. 1527-1532.

Carrington, C. G., Liu, Q., (1995). Calorimeter measurements of a heat pump dehumidifier: influence of evaporator air flow. *International journal of energy research,* v. 19, p. 649-658.

Gad, H. E., Hamed, A. M., El-Sharkawy, I. I., (2001). Application of a solar desiccant/collector system for water recovery from atmospheric air. *Renewable Energy* v. 22, p. 541-556.

Ghaffour, N., Missimer, T. M., Amy, G. L., (2013). Technical review and evaluation of the economics of water desalination: Current and future challenges for better water supply sustainability. *Desalination* v. 309, p . 197-207.

Gleick, P. H., (2000). A look at twenty-first century water resources development. *Water International* v. 25, p. 127-138.

Gleick, P. H., (1996). Water resources. In *Encyclopedia of Climate and Weather,* Vol. 2, edited by S. H. Schneider. New York: Oxford University Press.

Habeebullah, B. A., (2009). Potential use of evaporator coils for water extraction in hot and humid areas. *Desalination* v. 237, p. 330-345.

Helmreich, B., Horn, H., (2009). Opportunities in rainwater harvesting. *Desalination* v. 248, p. 118-124.

Ji, J. G., Wang, R. Z., Li, L. X., (2007). New composite adsorbent for solar-driven fresh water production from the atmosphere. *Desalination* v. 212, p. 176-182.

Jradi, M., Ghaddar, N., Ghali, K., (2012). Experimental and theoretical study of an integrated thermoelectric–photovoltaic system for air dehumidification and fresh water production. *International Journal of Energy Research* v. 36, p. 963-974.

Khalil, A., (1993). Dehumidification of atmospheric air as a potential source of fresh water in the UAE. *Desalination* v. 93, p. 587-596.

Mezher, T., Fath, H., Abbas, Z., Khaled, A., (2011). Techno-economic assessment and environmental impacts of desalination technologies. *Desalination* v. 266, p. 263-273.

Milani, D., Abbas, A., Vassallo, A., Chiesa, M., Bakri, D. A., (2011). Evaluation of using thermoelectric coolers in a dehumidification system to generate freshwater from ambient air. *Chemical Engineering Science* v. 66, p. 2491-2501.

Miller, J. E., (2003). *Review of water resources and desalination technologies*. Albuquerque: Sandia National Laboratories - Unlimited Release.

Narayan, G. P., Sharqawy, M. H., Summers, E. K., Lienhard, J. H., Zubair, S. M., Antar, M. A., (2010). The potential of solar-driven humidification–dehumidification desalination for small-scale decentralized water production. *Renewable and Sustainable Energy Reviews* v. 14, p. 1187-1201.

Scrivani, A., Bardi, U., (2008). A study of the use of solar concentrating plants for the atmospheric water vapour extraction from ambient air in the Middle East and Northern Africa region. *Desalination* v. 220, p. 592-599.

Shanmugam, G., Jawahar, G. S., Ravindran, S., (2004). Review on the Uses of Appropriate Techniques for Arid Environment. In *Proceedings of International Conference on Water Resources and Arid Environment*, Riyadh, Saudi Arabia.

Starr, V. P., (1972). Controlled atmospheric convection in an engineered structure. *Nordic Hydrology* v. 3 p. 1-21.

United Nations, (2013). *The Millennium Development Goals Report 2013*. New York: United Nations.

Vián, J. G., Astrain, D., Domınguez, M., (2002). Numerical modelling and a design of a thermoelectric dehumidifier. *Applied Thermal Engineering* v. 22 p. 407-422.

Wahlgren, R. V., (2001). Atmospheric water vapour processor designs for potable water production: a review. *Water Research* v. 35, p. 1-22.

Appendix A. NOMENCLATURE.

Latin Letters

A	inflow pipe section, m^2
c	specific heat, J/kg°C
f	conversion factor
F	bypass factor
M	mass, g
m	molar mass, g/mol
n	moles number, mol
P	pressure, mbar
Q	heat, W
$\dot{q}$	condensed water flow, l/h
R	universal gas constant, J/K mol
r	evaporation latent heat, kJ/kg
RP	refrigeration power, W
S	air flow speed, m/s
T	temperature, °C
V	air and water vapor mixture volume
$\dot{v}$	volumetric air flow, m^3/h

Greek Letters

ρ	density, kg/m^3
ω	absolute humidity, $g_{H2O}/kg_{dry\ air}$

Subscripts

a	atmospheric state
air	air
c	post-evaporator state
e	heat exchanger exit state
H2O	water
l	latent
s	sensible

Appendix B. AWVP MODEL PARAMETER VALUES.

Parameter	Value	Unit of measure
A	0.0007	-
B	0.00000346	-
c_{air}	1005	J/kg°C
f	1000	g_{H2O}/kg_{H2O}
m_{air}	28.84	g/mol
m_{H2O}	18.016	g/mol
R	8.3144	J/mol K
r_{H2O}	2272	kJ/kg
x	6.1121	-
y	17.123	-
z	234.95	-
ρ_{H2O}	1	kg/l